A Novel Framework for Virtual Prototyping of Rehabilitation Exoskeletons

Priyanshu Agarwal, Pei-Hsin Kuo, Richard R. Neptune, and Ashish D. Deshpande
Department of Mechanical Engineering
The University of Texas at Austin
Austin, TX 78712
Email: mail2priyanshu@utexas.edu

***Abstract*—Human-worn rehabilitation exoskeletons have the potential to make therapeutic exercises increasingly accessible to disabled individuals while reducing the cost and labor involved in rehabilitation therapy. In this work, we propose a novel human-model-in-the-loop framework for virtual prototyping (design, control and experimentation) of rehabilitation exoskeletons by merging computational musculoskeletal analysis with simulation-based design techniques. The framework allows to iteratively optimize design and control algorithm of an exoskeleton using simulation. We introduce biomechanical, morphological, and controller measures to quantify the performance of the device for optimization study. Furthermore, the framework allows one to carry out virtual experiments for testing specific "what-if" scenarios to quantify device performance and recovery progress. To illustrate the application of the framework, we present a case study wherein the design and analysis of an index-finger exoskeleton is carried out using the proposed framework.**

I. Introduction

Human-worn robotic exoskeletons provide a promising avenue for assisting stroke patients to recover motor function and for easing the burden of labor intensive, highly repetitive, and therefore, costly conventional physical therapy. Clinical trials have shown that robot-aided therapy results in improved limb motor function after chronic stroke with increased sensorimotor cortex activity for practiced tasks [1], [2], [3], [4]. Design of robotic exoskeletons is challenging due to the limits on size and weight, and the need to address technical challenges in areas ranging from biomechanics, rehabilitation, actuation, sensing, physical human-robot interaction, and control based on the user intent [5], [6], [7]. The process involves design of the robot hardware including selection of the robot architecture, method for attachment to the wearer, choice of design parameters, and the control system design. Since the exoskeletons are in close physical contact with the subjects, a synergistic approach that accounts for the coupled human-robot system is needed.

To generate effective exoskeleton designs, our goal is to develop design and analysis tools that allow for simultaneous modeling of the robot hardware and subject's musculoskeletal biomechanics. For engineering design applications, simulation-based design methodologies have been developed that achieve iterative refinements of the product models early in the design stage to develop more cost- and time-effective products with superior performance and quality [8]. Recently, a few tools such as Software for Interactive Musculoskeletal Modeling (SIMM) [9], OpenSim [10], AnyBody Modeling System [11], LifeModeler [12], Virtual Interactive Musculoskeletal System (VIMS) [13] have been developed for musculoskeletal analysis. However, computational tools in biomechanics have not been effectively combined with traditional engineering design techniques. In the past, a few attempts have been made to simulate a combined human-exoskeleton system using musculoskeletal analysis [14], [15]. However, a systematic framework for quantitative evaluation of competing alternatives, and a mechanism for parametric design refinement via studying the effects of exoskeletons on human musculoskeletal system and the control algorithm development is currently missing.

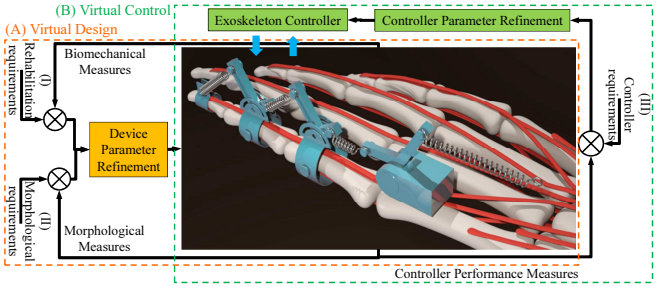

Fig. 1. Virtual prototyping framework illustrating the virtual design and control of an index finger exoskeleton using biomechanical, morphological, and controller performance measures. (Best viewed in color)

In this work, we propose a human-model-in-the-loop framework which merges the computational musculoskeletal analysis with simulation-based design methodologies. The objective of this framework is to carry out *virtual prototyping* of the rehabilitation exoskeletons. The framework allows for iterative optimization of exoskeletons using biomechanical, morphological and controller performance measures. Furthermore, it allows for carrying out virtual experimentation for testing specific "what-if" scenarios to quantify device performance and recovery progress. To illustrate the development and application of the framework, we present a case study wherein virtual prototyping of an index-finger exoskeleton is carried out based on the relevant performance measures. Also, a "what-if" scenario is simulated using virtual experimentation to illustrate quantification of the recovery progress.

II. Virtual Prototyping Framework

We propose a novel framework to develop and refine hardware design and control algorithms for robotic systems that work in intimate contact of the human user. We introduce

978-1-4673-6024-1/13/$31.00 ©2013 IEEE

three types of measures to assess performance of the coupled human- exoskeleton model: (I) Biomechanical measures that include the measures from the musculoskeletal model (e.g. joint reaction forces, muscle forces, and metabolic power consumption etc.), (II) Morphological measures that are derived from the physical design (e.g. structure, link lengths, stiffness etc.) of the exoskeleton (e.g. coupled system range of motion, stability, controllability etc.), and (III) Controller measures that describe the performance of the exoskeleton controller (e.g. steady-state tracking error, response time, maximum overshoot etc.).

The following steps summarize the proposed framework (Fig. 1):

Step 1. Initial Modeling: Develop an initial coupled exoskeleton-limb musculoskeletal model, a controller for the exoskeleton and identify appropriate models for the sensors and actuators.

Step 2. Performance Measure Identification: Identify the key biomechanical, morphological, and controller performance measures. In addition, identify a nominal motion trajectory for the coupled exoskeleton-limb model based on the desired rehabilitation movement.

Step 3. Model Fidelity Improvement: Improve the coupled model fidelity by optimizing model parameters based on experimental measurements for the parameters of the human limb and the exoskeleton device.

Step 4. Virtual Design: Carry out virtual design by iteratively optimizing biomechanical and/or morphological performance measures while reproducing the nominal motion trajectory. This includes studying the effects of variability, determining the best geometries for performance (e.g. lower torques with improved controllability), and examining relationships between form and function (e.g. improved biomechanical compatibility). We plan to capitalize on setting up the design optimization problem by coupling parametric models with functional simulation tools.

Step 5. Virtual Control: Carry out virtual control by iteratively developing and refining control algorithms for the coupled system and optimizing the controller performance measures while tracking the desired motion trajectory using the designed exoskeleton controller.

Step 6. Virtual Experimentation: Carry out virtual experiments to study specific "what-if" scenarios (e.g. certain dysfunctional muscles in a patient) and generate modifications in the design and control to help address such cases.

We believe that the proposed framework can help quantify the performance of many candidate designs, and thus significantly shorten the development life cycle of exoskeletons.

III. Index Finger Exoskeleton Prototyping Case Study

In this section, we present a case study to illustrate the application of the proposed framework to virtual prototype an index finger exoskeleton. We also present a virtual experimentation scenario where improving rehabilitation is simulated. Fig. 2(a) presents a preliminary prototype of the device. The setup consists of a base to which the exoskeleton and the actuators (not shown in figure) are connected. The design supports active assistance of the finger joints degrees of freedoms (DOFs) in both flexion and extension and has an unactuated

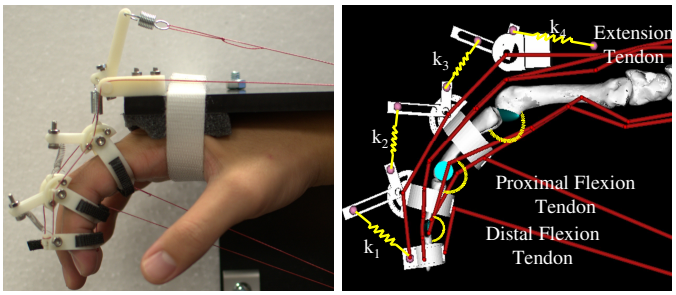

(a) (b)

Fig. 2. Finger-exoskeleton coupled system. (a) Preliminary 3D printed prototype of the device, and (b) virtual prototype (musculoskeletal model) used for the simulations. The model has 6 degrees of freedom consisting of index finger metacarpophalangeal (MCP) flexion, proximal interphalangeal (PIP) flexion, distal interphalangeal (DIP) flexion, and exoskeleton proximal, middle, distal link rotation. The 3 exotendons Distal Flexion Tendon (TFD), Proximal Flexion Tendon (TFP), and Extension Tendon (TE) were also modeled as muscles. The four finger muscles in the model were Flexor Digitorum Profundus (FDP), Flexor Digitorum Sublimis (FDS), Extensor Digitorum Communis (EDC), and Extensor Indicis Proprius (EIP). (Best viewed in color)

DOF for abduction and adduction at the metacarpophalangeal (MCP) joint. The device is actuated using three exotendons (two flexion and one extension). The design has a mechanism to adjust the lengths of the links to accommodate variation in different hand sizes. The range of motion of various joints can also be adjusted as per patients' rehabilitation needs. We introduce spring elements as links in the design, in addition to the size adjusting mechanism to: (1) develop a more kinematically and dynamically compatible exoskeleton by exploiting its passive dynamics for effective therapy; and (2) help accommodate axis misalignment leading to reduced undesired reaction forces at the human joints. The design has passive stiffness at each joint with antagonistic tendon driven actuation making the design passively dynamic and allowing for conformation with the hand joint axes of rotation.

We use OpenSim [10] as the computational engine to carry out the musculoskeletal analysis. The OpenSim musculoskeletal model is built up as a constrained articulated multibody system with rigid skeletal body segments overlaid with multiple muscles that serve to actuate the system. The elements of the musculoskeletal system are modeled by musculoskeletal geometry, constrained multibody segmental dynamics, and a set of differential equations that describe muscle contraction dynamics. OpenSim allows for monitoring of a number of internal human variables including system lengths, actuator forces, reactions at joints, and mechanical work.

A. Initial Modeling

To develop a coupled index-finger-exoskeleton model, an index-finger musculoskeletal model (Fig. 3b) was isolated from the upper extremity model (Fig. 3a) described by Holzbaur et al. [16] while retaining the wrapping surfaces and 4 Hill-type musculotendon actuators associated with the index finger. A coupled finger-exoskeleton model (Fig. 2(b)) was developed to closely resemble the preliminary prototype of the device using this isolated model. A linear passive rotational stiffness element was added at the 3 index finger joints to represent the passive torques due to ligaments and other structures. Also, linear spring elements (k_1-k_4) coupling the various exoskeleton

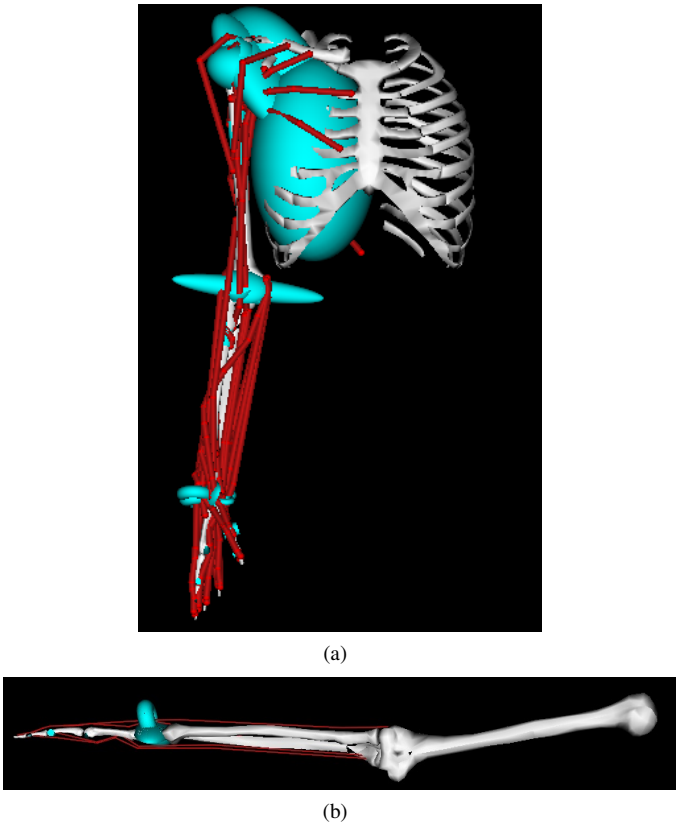

(a)

(b)

Fig. 3. Musculoskeletal model of the human upper limb. (a) Stanford VA Upper Limb Model and (b) isolated index finger model. (Best viewed in color)

links were added to the model. We treated the 3 exotendons as the force generating elements and modeled them as muscle-tendon units with their optimal fiber length chosen such that the actuators can generate wide range of forces over the exotendon excursions corresponding to the range of motion for the finger joints.

B. Performance Measure Identification

We assessed the performance using the following measures: (1) Biomechanical measures - consisting of joint reaction forces which are important biomechanical factors for a hand exoskeleton; and (2) Morphological measures - quantifying exoskeleton kinematic and dynamic compatibility in terms of nominal motion tracking performance, which are governed by the stiffness combination of the exoskeleton.

We used a sinusoidal flexion-extension task expressed in (1) to be the nominal motion for the index finger joints and assumed the exoskeleton joint angular displacements to be zero as these are small during this motion. A relationship between proximal interphalangeal (PIP) and distal interphalangeal (DIP) joint angles, based on hand anatomy [17], was used to constrain the two joint angles.

$$\begin{aligned} \theta_j &= k_j \sin(\omega t), \;\; j \in \{MCP, PIP\} \\ \theta_{DIP} &= \frac{2}{3}\theta_{PIP} \end{aligned} \tag{1}$$

where θ_j and k_j represents the joint angle and scaling factor of j^{th} joint, respectively and ω represents the angular frequency.

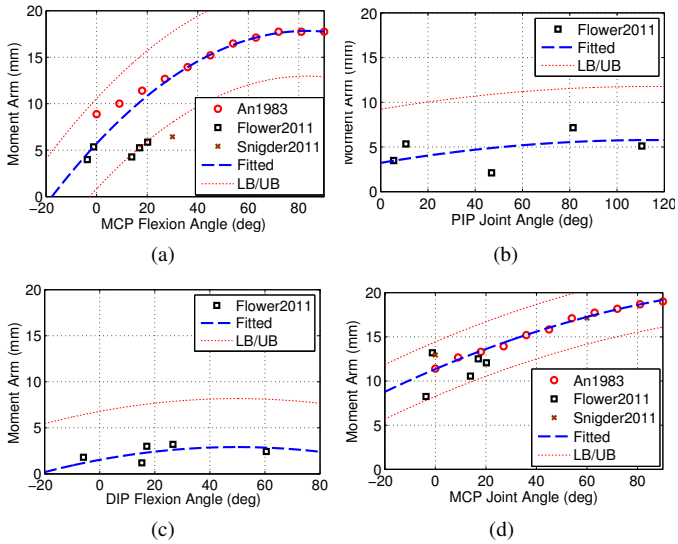

Fig. 4. The fitting results for the index finger flexors at the three joints of the index finger. Flexor Digitorum Profundus (FDP) muscle at (a) MCP, (b) PIP, (c) DIP, and (d) Flexor Digitorum Sublimis (FDS) muscle at MCP.

TABLE I. THE GOODNESS OF FIT STATISTICS FOR THE SECOND ORDER POLYNOMIAL FITTING OF THE INDEX FINGER MUSCLES MOMENT ARM DATA.

Fitting Function	FDP			FDS
	MCP	PIP	DIP	MCP
$\mathbf{R^2}$	0.92	0.78	0.75	0.95
RMSE (mm)	1.61	0.82	0.66	1.12

C. Model Fidelity Improvement

1) Moment Arm Experimental Data Fitting: Experimental results of the moment arms derived from cadaveric or in vivo studies vary among different studies due to differences in methodologies adopted and size of subjects or test specimens [18], [19], [20], [21]. In order to evaluate accurate moment arms for the adopted model, the experimental data was first normalized and then fitted with a second order polynomial function. We normalized the moment arm data by multiplying it with a ratio of the total index finger length of the isolated model to the length provided in the respective data set. We only evaluate moment arm fitting functions for the index finger flexors–Flexor Digitorum Profundus (FDP) at MCP, PIP, and DIP and Flexor Digitorum Sublimis (FDS) at MCP, due to the availability of reliable data for these muscles at the specified joints. Fig. 4 presents the scaled moment arm data along with the fitted data for the adopted model. The fitting results (Table I) show that the nonlinear fitting functions have statistical robustness to represent the experimental moment arm data.

2) Muscle Moment Arm Optimization: A comparison of the muscle moment arm of the available model with the fitted data (Fig. 4) showed that the two differ significantly. Previously, a study has optimized the shoulder joint moment arms by altering the wrapping object parameters [22]. However, no study has optimized the moment arms by altering both the muscle origin/via/insertion points and the wrapping object parameters. We used optimization techniques to refine the

moment arm of each muscle individually by altering both the muscle points and the wrapping object parameters to minimize the difference between model and experimentally fitted moment arms (2) subjected to upper (ϵ) and lower limits ($-\epsilon$) on the allowable changes ($X - X_0$) in the parameters.

$$\begin{aligned} &\underset{X}{\text{minimize}}\ J(X) = \sum_{i=1}^{m}\left[\sum_{j=1}^{n}[f_{\text{mod}}(\theta_{ij}, X) - f_{\text{exp}}(\theta_{ij})]^2\right] \\ &\text{subject to}\ -\epsilon \leq X - X_0 \leq \epsilon \end{aligned} \tag{2}$$

where m is the number of joints spanned by the muscle, n is the number of time steps, θ_{ij} is the joint angle of the i^{th} joint at the j^{th} time step, X is the location of origin/via/insertion points.The dimensions of the wrapping objects, f_{mod} and f_{exp}, are the model determined and experimentally measured moment arms, respectively. We evaluated the moment arms using OpenSim and employed an interior-point algorithm [23] for optimization. The MATLAB-OpenSim interface developed to carry out the optimization of the different muscles in the model is described next.

3) MATLAB-OpenSim Framework Overview: Fig. 5 presents an overview of the developed MATLAB-OpenSim framework. A MATLAB script writes an OpenSim model file and states (joint angles) file with the desired model parameters and states, respectively. The OpenSim API commands are then invoked from within MATLAB to analyze and output the moment arm of each muscle in the model for the specified states to results files. The results files and the fitted results (Fig. 4) are used to evaluate the optimization objective function (Eq. 2). The model parameters are iteratively optimized based on the objective function value. Currently, the developed framework is geared towards optimizing the moment arm. However, the OpenSim API commands can be used to carry out different types of analyses using the corresponding API commands.

D. Virtual Design

For the coupled optimized model to reproduce the nominal trajectory for virtual design, we carried out a Computed Muscle Control (CMC) analysis in OpenSim. CMC is an efficient algorithm to compute muscle excitation patterns using static optimization along with feedforward and feedback control to drive the kinematic trajectory of a musculoskeletal model towards a set of desired kinematics [24]. We use the nominal motion expressed in (1) to be the desired motion for the coupled system ($\ddot{q}_j^*$, $\ddot{q}_k^*$) and impose constraints on the maximum allowable excitation (u_i) of the index finger muscles to simulate a pathological finger as in (3). Also, lower tracking weights ($w_{\text{exo}} << w_{\text{fin}}$) for exoskeleton link joint angles and reserve actuators at the various joints were used to compensate for the assumed motion of the exoskeleton links.

$$\begin{aligned} \underset{u_i}{\text{minimize}} \quad & J(u_i) = \sum_{i=1}^{7} u_i^2 + \sum_{j=1}^{3} w_{\text{fin}}(\ddot{q}_j^* - \ddot{q}_j)^2 \\ & + \sum_{k=1}^{3} w_{\text{exo}}(\ddot{q}_k^* - \ddot{q}_k)^2 \\ \text{subject to} \quad & u_i \leq u_{max},\ 1 \leq i \leq 7 \end{aligned} \tag{3}$$

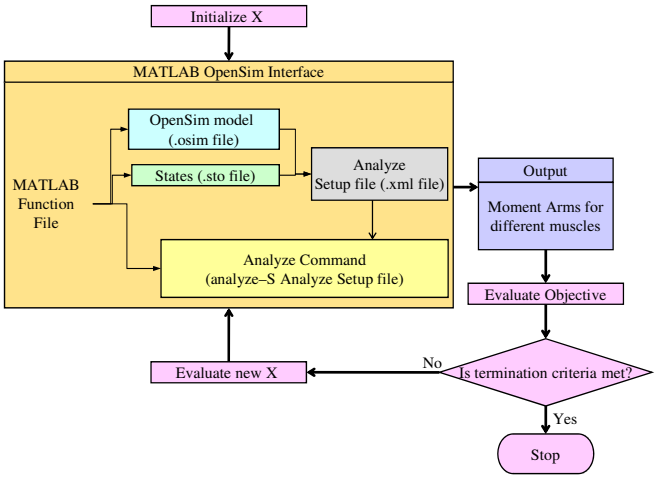

Fig. 5. The developed MATLAB-OpenSim interface for moment arm optimization. An OpenSim model was generated on-the-fly using MATLAB with the initial parameters. The model was then analyzed for the moment arms using the OpenSim API commands from within MATLAB. The resulting moment arms were used to evaluate the objective function and the model optimized iteratively till the termination criteria were met.

In this case study, we focus on the appropriate choice of the exoskeleton stiffness that would result in best tracking performance with the least joint reaction forces, while obtaining the required muscle excitation using CMC. To this end, we carried out a parametric study to assess the effect of the exoskeleton spring stiffness (k_1-k_4) on tracking performance and joint reaction forces using CMC analysis.

E. Virtual Experimentation: Simulating Improving Rehabilitation

A "what-if" study was carried out to assess whether a recovering finger can be simulated which is helpful in quantifying the recovery progress. Improved finger condition was simulated by increasing the maximum allowable excitation (u_{max}) constraint (3) on finger muscles during CMC and evaluating the required muscle and exotendon forces. Since, with this new constraint higher excitations are allowed for the finger muscles, a redistribution of the forces in the muscles and exotendons takes place with more forces being applied by the finger muscles. By feeding in the exotendon forces measured on the actual prototype into the developed model, the forces applied by the finger muscles can be determined and thus, rehabilitation improvement can be quantified. In addition, the model can be used to determine the actuation requirement under different rehabilitation conditions.

IV. Results

A. Model Fidelity Improvement

Fig. 6 shows the optimized model moment arm comparison with the fitted (experimentally measured) data for the FDP muscle at the MCP, PIP, and DIP joints. It can be seen that the initial model based moment arms were significantly different from the fitted (measured) data. However, after optimization the model based estimates were close to the fitted data. Fig. 7 shows the OpenSim model before and after the optimization of the moment arms.

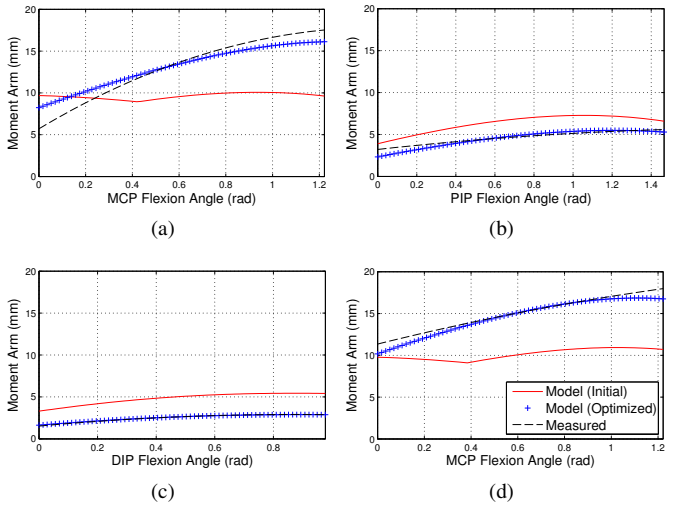

Fig. 6. Optimized model moment arm comparison with the experimentally measured data for FDP muscle at (a) MCP joint, (b) PIP joint, (c) DIP joint and (d) FDS muscle at MCP joint.

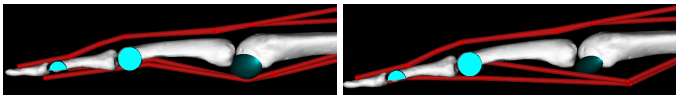

(a) Before (b) After

Fig. 7. Comparison of model before and after muscle moment arm optimization. Alterations in both the origin-, via-, insertion-points and wrapping object dimensions resulted in optimized muscle moment arms.

B. Virtual Design

1) Effect of Stiffness on Tracking Performance: Fig. 8 presents the tracking performance during CMC for the tracking task. The finger joint angles (MCP (CMC), PIP (CMC), DIP (CMC)) were very close to their respective nominal positions (MCP (Ref), PIP (Ref), DIP (Ref)). Lower exoskeleton stiffness resulted in large fluctuations in the exoskeleton links angular position (Exo Prox (CMC), Exo Mid (CMC), Exo Dist (CMC)). There was also a stiffness relationship among different exoskeleton links which was needed for kinematic and dynamic compatibility of the exoskeleton with the finger. Furthermore, increasing the stiffness of the exoskeleton resulted in better tracking of the joint angles as the exoskeleton joint angle fluctuations were reduced.

2) Effect of Stiffness on Joint Reaction Forces: Fig. 9 presents the induced reaction forces at the finger joints for the tracking task. Increasing exoskeleton stiffness resulted in an increase in the magnitude of the finger joint reaction forces throughout the duration of the task.

Results showed that for the current design, kinematics (joint motion tracking) is much more sensitive to the stiffness variation than the dynamics (joint reaction forces).

C. Virtual Experimentation: Simulating Improving Rehabilitation

Fig. 10 presents the active muscle fiber forces in two different (15% and 85%) recovery scenarios. It can be seen that the active finger muscle fiber forces (FDSI, FDPI, EDCI, EIP) are small. Furthermore, with increased recovery more

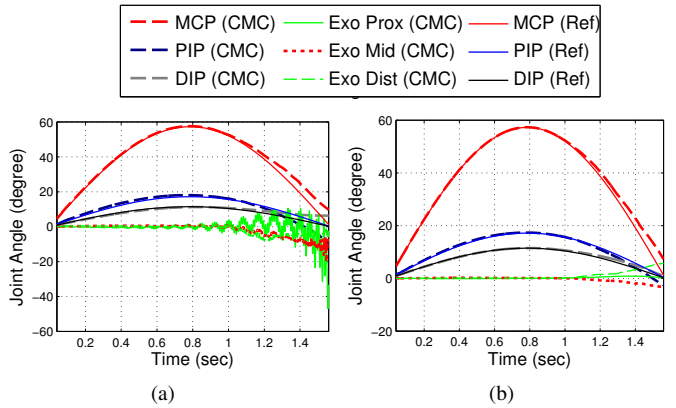

Fig. 8. Joint angle tracking performance for various joints in the system with different exoskeleton stiffness as obtained from the CMC analysis. (a) Low stiffness (k1 = 250, k2 = 275, k3 = 500, k4 = 600) N/m and (b) high stiffness (k1 = 800, k2 = 900, k3 = 1000, k4 = 1100) N/m. The exoskeleton links show large fluctuations at lower exoskeleton stiffness. Also, there is an appropriate relationship of stiffness among different links of the exoskeleton for kinematic and dynamic compatibility of the exoskeleton with the finger. Increasing exoskeleton stiffness resulted in improved tracking performance. (Best viewed in color)

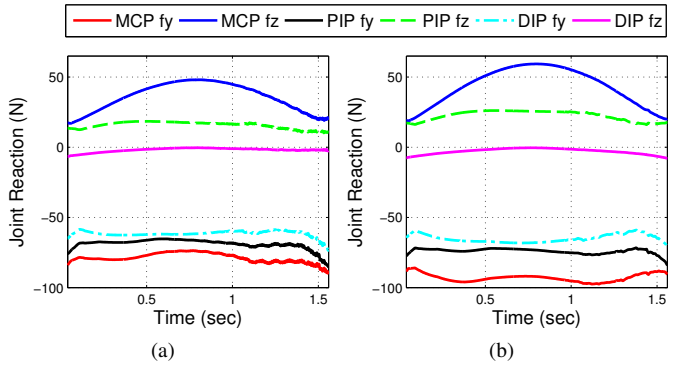

Fig. 9. Joint reactions induced at the various index finger joints with different exoskeleton stiffness as obtained from the CMC analysis. (a) Low stiffness (k1 = 250, k2 = 275, k3 = 500, k4 = 600) N/m and (b) high stiffness (k1 = 800, k2 = 900, k3 = 1000, k4 = 1100) N/m. (Best viewed in color)

forces were applied by the finger muscles (especially FDSI) as opposed to the exotendons (TFD, TE).

V. Conclusion

We presented a systematic framework for virtual prototyping of exoskeletons capitalizing on musculoskeletal simulations of a coupled exoskeleton-limb model. Successful simulation of the modeled coupled index finger-exoskeleton system showed that the proposed virtual prototyping framework is a powerful tool for designing, analyzing and experimenting with a virtual prototype while quantifying its performance. Specifically, the case study showed the successful modeling of the exotendons as muscle-tendon units in the developed coupled model of the index-finger exoskeleton. The optimization-based approach to modify muscle moment arms by altering the muscle path showed that model fidelity can be improved using experimental measurements. Furthermore, the parametric study carried out for the design variables using CMC showed that the kinematics of the current design is more sensitive to changes in stiffness than its dynamics. Finally, the virtual experiment

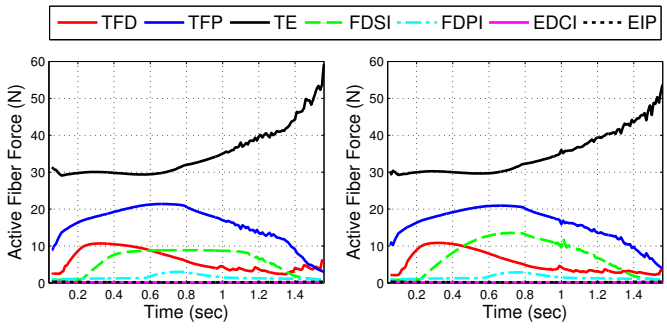

Fig. 10. Active muscle fiber forces in two simulations representing the improving rehabilitation scenario. (a) 15% recovery and (b) 85% recovery from complete motor disability. Different rehabilitation scenarios are simulated by changing the constraint on the maximum allowable excitation of the index finger muscles. With increased recovery more forces are applied by the finger muscles. (Best viewed in color)

carried out to simulate improving rehabilitation showed that a quantification of the rehabilitation process is possible using the current framework.

In the future, we plan to integrate the framework with OpenSim by appending OpenSim functionality (using C++ classes) to allow for modeling robotic elements more accurately. Specifically, we plan to develop a new type of tendon-driven series elastic actuator for accurately modeling actuation in robotic devices that interact with the human body. Such an actuator would explicitly capture the kinematics and dynamics of the exotendons for accurate virtual control simulation. Furthermore, we plan to develop a non-linear stiffness element which can capture the non-linear passive torque-angle relationship at the human finger joints accurately. Using such a framework, a design optimization study can be carried out with other exoskeleton design parameters including mechanism structure and dimensions of various links. A quantitative metric based on tracking performance, required exotendon forces, and induced joint reaction forces can be developed to assess the performance of candidate exoskeleton designs. Finally, the chosen exoskeleton stiffness can be used to build a prototype and motion capture data collected on the actual device to simulate the coupled system with the actual data and further improve the performance of the device.

ACKNOWLEDGMENT

This work was supported, in part, by the National Science Foundation (NSF) grant #NSF-CPS-1135949. The contents are solely the responsibility of the authors and do not necessarily represent the official views of the NSF.

REFERENCES

[1] G. Prange, M. Jannink, C. Groothuis-Oudshoorn, H. Hermens, and M. Ijzerman, "Systematic review of the effect of robot-aided therapy on recovery of the hemiparetic arm after stroke," *Journal of rehabilitation research and development*, vol. 43, no. 2, pp. 171–184, 2006.

[2] C. D. Takahashi, L. Der-Yeghiaian, V. Le, R. R. Motiwala, and S. C. Cramer, "Robot-based hand motor therapy after stroke," *Brain*, vol. 131, no. 2, pp. 425–437, 2008.

[3] P. Langhorne, F. Coupar, and A. Pollock, "Motor recovery after stroke: a systematic review," *Lancet neurology*, vol. 8, no. 8, pp. 741–754, 2009.

[4] C. H. Hwang, J. W. Seong, and D. S. Son, "Individual finger synchronized robot-assisted hand rehabilitation in subacute to chronic stroke: a prospective randomized clinical trial of efficacy," *Clinical Rehabilitation*, vol. 26, no. 8, pp. 696–704, 2012.

[5] A. Dollar and H. Herr, "Lower extremity exoskeletons and active orthoses: Challenges and state-of-the-art," *IEEE Transactions on Robotics*, vol. 24, no. 1, pp. 144–158, 2008.

[6] H. Hugh, "Exoskeletons and orthoses: classification, design challenges and future directions," *Journal of NeuroEngineering and Rehabilitation*, vol. 6, pp. 1–21.

[7] P. Heo, G. Gu, S. Lee, K. Rhee, and J. Kim, "Current hand exoskeleton technologies for rehabilitation and assistive engineering," *International Journal of Precision Engineering and Manufacturing*, vol. 13, no. 5, pp. 807–824, 2012.

[8] G. Wang, "Definition and review of virtual prototyping," *Journal of Computing and Information Science in Engineering (Transactions of the ASME)*, vol. 2, no. 3, pp. 232–236, 2002.

[9] MusculoGraphics, Inc., "Musculographics, musculographics SIMM software suite," http://www.musculographics.com.

[10] S. Delp, F. Anderson, A. Arnold, P. Loan, A. Habib, C. John, E. Guendelman, and D. Thelen, "Opensim: open-source software to create and analyze dynamic simulations of movement," *IEEE Transactions on Biomedical Engineering*, vol. 54, no. 11, pp. 1940–1950, 2007.

[11] AnyBodyTechnology, "The AnyBody modeling system," http://www.anybodytech.com.

[12] LifeModeler, Inc., "LifeModeler," http://www.lifemodeler.com.

[13] C. Edmund, A. Robert, Y. Hiroaki, L. Jonathan, and H. Naoki, "Virtual interactive musculoskeletal system (vims) in orthopaedic research, education and clinical patient care," *Journal of Orthopaedic Surgery and Research*, vol. 2, no. 1, 2007.

[14] P. Agarwal, M. Narayanan, L. Lee, F. Mendel, and V. Krovi, "Simulation-based design of exoskeletons using musculoskeletal analysis," in *ASME International Design Engineering Technical Challenges and Computers and Information in Engineering Conference*, 2010, pp. 1357–1364.

[15] K. Cho, Y. Kim, D. Yi, M. Jung, and K. Lee, "Analysis and evaluation of a combined human exoskeleton model under two different constraints condition," in *Proceedings of the International Summit on Human Simulation*, 2012.

[16] K. Holzbaur, W. Murray, G. Gold, and S. Delp, "Upper limb muscle volumes in adult subjects," *Journal of biomechanics*, vol. 40, no. 4, pp. 742–749, 2007.

[17] H. Rijpkema and M. Girard, "Computer animation of knowledge-based human grasping," in *ACM SIGGRAPH Computer Graphics*, vol. 25, no. 4, 1991, pp. 339–348.

[18] K. An, Y. Ueba, E. Chao, W. Cooney, and R. Linscheid, "Tendon excursion and moment arm of index finger muscles," *Journal of Biomechanics*, vol. 16, no. 6, pp. 419–425, 1983.

[19] N. Fowler, A. Nicol, B. Condon, and D. Hadley, "Method of determination of three dimensional index finger moment arms and tendon lines of action using high resolution mri scans," *Journal of Biomechanics*, vol. 34, no. 6, pp. 791–797, 2001.

[20] J. Martin, M. Latash, and V. Zatsiorsky, "Effects of the index finger position and force production on the flexor digitorum superficialis moment arms at the metacarpophalangeal jointsa magnetic resonance imaging study," *Clinical Biomechanics*, vol. 27, no. 5, pp. 453–459, 2012.

[21] J. Snijders, J. Visser, J. Korstanje, R. Selles, and H. Veeger, "Estimation of in-vivo muscle moment arms around the mcp joint using ultrasound," Master's thesis, Delft University of Technology, 2011.

[22] C. Gatti and R. Hughes, "Optimization of muscle wrapping objects using simulated annealing," *Annals of biomedical engineering*, vol. 37, no. 7, pp. 1342–1347, 2009.

[23] R. Byrd, M. Hribar, and J. Nocedal, "An interior point algorithm for large-scale nonlinear programming," *SIAM Journal on Optimization*, vol. 9, no. 4, pp. 877–900, 1999.

[24] D. Thelen and F. Anderson, "Using computed muscle control to generate forward dynamic simulations of human walking from experimental data," *Journal of biomechanics*, vol. 39, no. 6, pp. 1107–1115, 2006.